Contribution from the Département de Recherche Fondamentale, Service de Physique, Centre d'Etudes Nucléaires, 85X 38041 Grenoble Cedex, France, and Department of Inorganic Chemistry, University of Nijmegen, Toernooiveld, 6525 ED Nijmegen, The Netherlands

# Electrochemistry and EPR Studies of $[Fe_4(\mu_3\text{-}S)_3(\mu_3\text{-}S_2)Cp_4]$, a Tetranuclear Metal Cluster That Reversibly Attains Five Oxidation States

J. Jordanov,[†‡] J. Gaillard,[†] M. K. Prudon,[§] and J. G. M. van der Linden*[§]

*Received September 9, 1986*

The redox properties of $[Fe_4S_5Cp_4]^n$ have been investigated in acetonitrile by using pulse and cyclic voltammetric techniques. At a platinum electrode three single-electron-oxidation and two single-electron-reduction processes were observed for the neutral compound ($n = 0$). The appearance of essentially the same $i$–$E$ curves for the 1+ and 2+ cluster ions assessed the chemical reversibility of the oxidation processes. The first reduction process was reversible only at lower temperatures (240 K) whereas the second reduction remained irreversible. At a mercury electrode only two single-electron-oxidation processes were observed, because of the accessible potential range, and one irreversible two-electron-reduction process was observed. The EPR spectra, recorded at 40 K, of the paramagnetic odd-electron-number cluster ions ($n = 3+, 1+, 1-$), showed $g$ values characteristic of an overall electron spin state $S = {}^1/_2$. The existence of $[Fe_4S_5Cp_4]^n$ at six different oxidation states ($n = 2-$ to 3+), of which five ($n = 1-$ to 3+) keep the cluster structure intact, is discussed in relation to molecular structure variations.

## Introduction

Continuing interest in iron–sulfur multinuclear complexes arises from the known presence of such metal clusters at the active sites of larger iron–sulfur proteins, where they may ensure electron-transfer reactions.[1] In a general sense, metal clusters are regarded as "electron reservoirs", which can gain or loose several electrons without molecular disruption.[2] It is therefore possible to perform electrochemical studies in order to gain some insight as to how the addition or subtraction of electrons will affect the structural and electronical configurations. Indeed, some comparative structural analyses have been reported for the $[Fe_4S_4Cp_4]^n$ ($n =$ 0 to 4+),[2,3] the $[Fe_4S_4(NO)_4]^n$ ($n = 2-$ to 0),[4] and the $[Fe_4S_4(SR)_4]^n$ ($n = 2-, 3-$)[5] redox series.

Earlier we reported a distorted cubane-like $Fe_4S_5$ core in the mono- and dication of the sulfur-rich cluster $[Fe_4S_5Cp_4]$ (Cp = $\pi$-cyclopentadienyl).[6,7] The distortion is brought about by the replacement, on one of the four edges, of a triply bridging sulfur by a quadruply bridging disulfide group. As a consequence, a pentacoordinated Fe site is present (bound to four S atoms and one Cp group) having no bonding interaction with the other four iron atoms.

Previous cyclic voltammetric studies by Vergamini and Kubas[8] showed that $[Fe_4S_5Cp_4]$ is sequentially oxidized in three one-electron steps. In this paper we report the detailed electrochemical characterization of $[Fe_4S_5Cp_4]$, by means of cyclic voltammetry and controlled-potential electrolysis at Pt and Hg electrodes. Two new, previously undetected, one-electron-reduction waves are proven to exist, and the following redox series is established: $[Fe_4S_5Cp_4]^{2-} \leftarrow [Fe_4S_5Cp_4]^- \rightleftarrows [Fe_4S_5Cp_4] \rightleftarrows [Fe_4S_5Cp_4]^+ \rightleftarrows [Fe_4S_5Cp_4]^{2+} \rightleftarrows [Fe_4S_5Cp_4]^{3+}$, where five oxidation states are reversibly available to the system. EPR studies have been performed to further identify and characterize the three paramagnetic states of the $[Fe_4S_5Cp_4]^n$ series ($n = 1-, 1+, 3+$).

## Experimental Section

**Measurements.** Electrochemical measurements were made with a potentiostat, PAR Model 173, equipped with an I/E converter, PAR Model 176, and coupled to a universal programmer, PAR Model 175. Normal- and differential-pulse voltammograms were obtained with a polarographic analyzer, PAR Model 174A, at a scan rate of 5 mV/s with a pulse frequency of 2.0 pulses/s (Pt electrode) or a drop time of 0.5 s (Hg electrode); the differential pulse amplitude was 25 mV. The recording devices were a Kipp BD30 recorder, a Tectronix 564 B storage oscilloscope, and a Nicolet Explorer II Model 206. Controlled-potential electrolytes were carried out with a Wenking LB 75M potentiostat and a Birtley electronic integrator. A conventional three-electrode system was used with either a platinum-disk working electrode or a mercury working electrode, PAR Model 303. The reference electrode was a silver wire immersed in a 0.1 M $AgNO_3$ solution in acetonitrile, separated from the test solution by a Luggin capillary containing the supporting electrolyte $Bu_4NPF_6$. This capillary was positioned as close as possible to the working electrode to minimize $iR$ drop, although also external $iR$ compensation was employed. All potentials reported herein are referred to the saturated calomel electrode and are uncorrected for liquid-junction potentials. A value of $E(Ag^+/Ag) - E(SCE) = 350$ mV was used, being the difference in half-wave potentials of ferrocene vs. these reference electrodes measured under the same experimental conditions. Measurements were made on approximately 1 mM solutions in acetonitrile. Controlled-potential electrolyses were made at potentials about 200 mV beyond the half-wave potential of the redox couple of interest, and they generated a sufficient concentration (0.5–1 mM) of the paramagnetic species. After the electrolyses had been completed, a sample was transferred under nitrogen into an EPR tube and then stored in liquid nitrogen until the EPR spectrum was recorded. All manipulations were carried out in a glovebox in which a dry and oxygen-free nitrogen atmosphere was maintained. EPR measurements were made on a Varian E109 spectrophotometer operating at ca. 9 GHz. Samples were cooled in a stream of helium gas, the temperature of which was regulated by an Oxford Instruments ESR 900 cryostat.

**Materials.** The cluster compounds $[Fe_4S_5Cp_4]^n$ ($n = 0, 1+, 2+$) were prepared as described previously.[8] The supporting electrolyte, $Bu_4NPF_6$ (obtained from Fluka), was recrystallized twice from ethanol and dried over $P_2O_5$ before use. Acetonitrile (Merck p.a.) was dried over molecular sieves (4 Å) and distilled over $CaH_2$ under nitrogen.

## Results and Discussion

The redox behavior of the $[Fe_4S_5Cp_4]^n$ ($n = 0, 1+, 2+$) cluster compounds was studied in acetonitrile at platinum and mercury electrodes vs. a $Ag^+/Ag$ reference electrode, by using normal- and differential-pulse techniques and cyclic voltammetry.

Table I summarizes the data from these electrochemical measurements, and in order to facilitate comparison with the literature, all potentials are referred to a SCE. (See Experimental Section.)

**Oxidations.** When starting with the neutral compound in solution, we observed three oxidations at a platinum electrode, two of which were also seen at the mercury electrode. The 2+/3+ oxidation reaction, at 1.19 V vs. SCE, is beyond the potential range

[†] Centre d'Etudes Nucléaires.
[‡] Also a member of the Centre National de la Recherche Scientifique.
[§] University of Nijmegen.

(1) (a) Lovenberg, W., Ed. *Iron-Sulfur Proteins*; Academic: New York, 1973, 1977 Vols. I and II, Vol. III. (b) Spiro, T. G., Ed. *Metal Ions in Biology*; Wiley-Interscience: New York, 1982; Vol. 4.
(2) Geiger, W. E.; Connelly, N. G. *Adv. Organomet. Chem.* **1985**, *24*, 87.
(3) Trinh-Toan; Teo, B. K.; Ferguson, J. A.; Meyer, T. J.; Dahl, L. F. *J. Am. Chem. Soc.* **1977**, *99*, 408.
(4) Chu, T. W. C.; Lo, F. Y. K.; Dahl, L. F. *J. Am. Chem. Soc.* **1982**, *104*, 3409.
(5) (a) Laskowski, E. J.; Reynolds, J. G.; Frankel, R. B.; Foner, S.; Papaefthymiou, G. C.; Holm, R. H. *J. Am. Chem. Soc.* **1979**, *101*, 6562. (b) Stephan, D. W.; Papaefthymiou, G. C.; Frankel, R. B.; Holm, R. H. *Inorg. Chem.* **1983**, *22*, 1550.
(6) Dupré, N.; Hendriks, H. M. J.; Jordanov, J.; Gaillard, J.; Auric, P. *Organometallics* **1984**, *3*, 800.
(7) Dupré, N.; Auric, P.; Hendriks, H. M. J.; Jordanov, J. *Inorg. Chem.* **1986**, *25*, 1391.
(8) Kubas, G. J.; Vergamini, P. J. *Inorg. Chem.* **1981**, *20*, 2667.

0020-1669/87/1326-2202$01.50/0 

**Table I.** Electrochemical Data for $[Fe_4S_5Cp_4]^n$ in Acetonitrile[a] (0.1 M $Bu_4NPF_6$)

| redox couple | temp, °C | normal-pulse voltammetry[b] $E_{1/2}$, V | slope,[c] mV | $i_d/C$, mA dm$^3$ mol$^{-1}$ | differential-pulse voltammetry[b] $E_p$, V | $w_{1/2}$,[e] mV | cyclic voltammetry $E_{1/2}$,[f] V | $\Delta E_p$,[g] mV | $i_b/i_f$ | $i_f/(Cv^{1/2})$, mA dm$^3$ s$^{1/2}$ mol$^{-1}$ V$^{-1/2}$ |
|---|---|---|---|---|---|---|---|---|---|---|
| | | | | Platinum Electrode | | | | | | |
| 2+/3+ | 20 | 1.19 | 61 | 0.19 | 1.19 | 102 | 1.19 | 65 | 1.01 | 0.15 |
| 1+/2+ | 20 | 0.07 | 54 | 0.19 | 0.07 | 100 | 0.07 | 60 | 0.93 | 0.14 |
| 0/+1 | 20 | −0.23 | 59 | 0.18 | −0.23 | 100 | −0.22 | 60 | 1.05 | 0.14 |
| 0/1− | 20 | −1.33 | 80[d] | 0.17 | −1.32 | 140 | −1.32 | | | 0.14 |
| | −30 | −1.42 | 87[d] | 0.05 | −1.42 | 120 | −1.42 | 140 | 0.93 | 0.04 |
| 1−/2− | 20 | −1.77 | 130 | 0.12 | −1.76 | 200 | −1.76[h] | | | 0.15 |
| | −30 | −1.76 | 100 | 0.05 | −1.72 | 200 | −1.87[h] | | | 0.04 |
| | | | | Mercury Electrode | | | | | | |
| 1+/2+ | 20 | 0.07 | 54 | 0.021 | 0.07 | 100 | 0.08 | 65 | 1.01 | 0.017 |
| 0/1+ | 20 | −0.22 | 60 | 0.021 | −0.22 | 100 | −0.22 | 65 | 1.07 | 0.016 |
| 0/2− | 20 | −1.27 | 65[d] | 0.048 | −1.26 | 210 | −1.34[h] | | | 0.056 |

[a] Potentials vs. SCE. [b] At a scan rate of 5 mV s$^{-1}$; pulse amplitude 25 mV. [c] Slope of the plot of $E$ vs. log $[(i_d - i)/i]$. [d] $E_{3/4} - E_{1/4}$. [e] Peak width at half-height. [f] At a scan rate of 100 mV s$^{-1}$; $E_{1/2} = {}^1/_2(E_{p,c} + E_{p,a})$. [g] $\Delta E_p$ is the cathodic–anodic peak potential separation. [h] Peak potential.

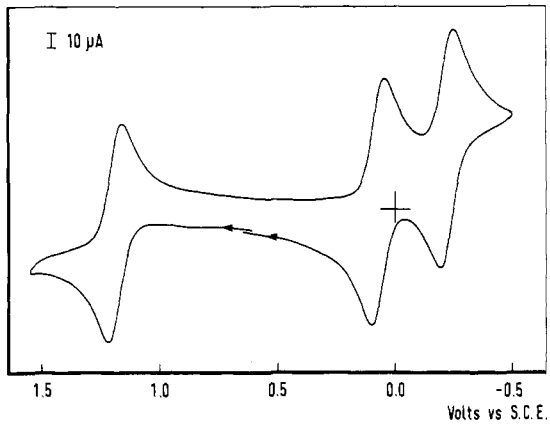


**Figure 1.** Redox behavior of the $Fe_4S_5Cp_4^{2+}$ compound (1 mM, 0.1 M $Bu_4NPF_6$) in acetonitrile at a platinum electrode in the potential range +1.55 to −0.50 V (vs. SCE) at a scan rate of 100 mV s$^{-1}$.

**Table II.** Fe–Fe Distances[a] (Å) and EPR Values for $Fe_4S_5Cp_4^n$

| | 3+ | 2+ | 1+ | 0 | 1− |
|---|---|---|---|---|---|
| | | | Distances | | |
| | | | X-rays | | |
| | | 2.650 | 2.723 | | |
| | | 2.661 | 2.866 | | |
| av | | 2.665 | 2.794 | | |
| | | | Fe-EXAFS | | |
| | | 2.63 | 2.65 | 2.61 | |
| | | 2.63 | 2.91 | 3.31 | |
| av | | 2.63 | 2.78 | 2.96 | |
| | | | EPR Values | | |
| $g_1$ | 2.083 | | 2.118 | | 2.041 |
| $g_2$ | 2.047 | | 1.999 | | 2.002 |
| $g_3$ | 1.977 | | 1.968 | | 1.987 |
| av | 2.036 | | 2.028 | | 2.010 |

[a] All the here given Fe–Fe distances occur only once.

of the mercury electrode which, under our conditions, proceeds until 0.60 V vs. SCE. These oxidation potentials were reported earlier[8] for dichloromethane solutions, but at 50 mV lower values, which is most probably caused by differences in the experimental conditions. Controlled-potential electrolysis for the oxidation of the 2+ cluster at 1.3 V revealed that one electron is transferred in this reaction. We conclude from the current functions ($i_d/C$ in pulse voltammetry and $i_f/(Cv^{1/2})$ in cyclic voltammetry) that in all redox reactions one electron is transferred.

Cyclic voltammetry shows that these oxidation reactions are chemically reversible, since well-resolved peaks were observed in the backward scan and $i_b/i_f$ ratios are all practically equal to 1. Also, other commonly applied criteria in the analysis of recorded $i$–$E$ curves, such as the slope of the linear log plot in PP and the width at half-height in DPP, point to reversible electron-transfer processes.

Starting with the mono- or dication cluster (Figure 1) in solution and performing the proper oxidation and reduction reactions for the 0/1+, 1+/2+, and 2+/3+ transitions, we obtained the same numerical values and essentially the same $i$–$E$ patterns. This confirms the chemical reversibility of these oxidation reactions.

**Adsorption of the 1+ Cluster Ion.** In cyclic voltammograms taken at a hanging-mercury-drop electrode, the oxidation wave of the monocation is accompanied by a postwave at $E_p = 0.1$ V. This postwave was observed either at higher scan rates (larger than 1 V/s) or at temperatures in the range from 273 to 240 K, and the intensity of the peak was proportional to the scan rate. A prewave was observed as well at the same potential by the reduction of the 2+ cluster ion. These phenomena indicate a reasonably strong adsorption of the monocation on a mercury surface.[9] This adsorption must be potential-dependent since no additional waves were observed with the 0/1+ and 1+/0 transitions. Some decomposition reactions seem to occur when the 1+ ion is oxidized, because some additional small oxidation peaks of adsorbed products were observed at 0.12 and 0.22 V and because a small reduction peak occurred at 0.17 V. At a platinum electrode, no such adsorption phenomena were observed in the cyclic voltammograms of the 1+ cluster ion.

**Reductions.** It has been reported[8] that $[Fe_4S_5Cp_4]$ does not exhibit any reduction waves. We do observe two reduction waves, however, when starting from the neutral compound as well as from the 1+ and 2+ compounds (Figure 2). These waves were exhibited at the platinum electrode, at −1.33 and −1.77 V vs. SCE, and they correspond to the monoanion and dianion formations, respectively. On the other hand, when a mercury electrode is used, the dianion is directly formed in a single step at −1.27 V vs. SCE. This conclusion is reached from the various current functions that indicate a two-electron-reduction process (see Table I). The negatively charged clusters are only formed when freshly distilled acetonitrile is used, most probably because they are reactive toward water.

At room temperature all these reduction processes are irreversible, since in the backward scans of the cyclic voltammograms no reoxidation waves were seen. Reversibility of the first reduction process at the platinum electrode can be achieved, however, by recording the cyclic voltammogram at lower temperatures (Figure 2 (bottom)). A peak is then gradually developed in the backward scan, until a well-resolved anodic wave is obtained at 243 K with $i_b/i_f = 0.9$. When this first reduction is followed (at 243 K) by

(9) Bard, A. J.; Faulkner, L. R. *Electrochemical Methods, Fundamentals and Applications*; Wiley: New York, 1980; Chapter 12.

**Table III.** Comparative Electrochemical Behavior of Iron-Sulfur Clusters ($E_{1/2}$ Values in Volts vs. SCE)

| compd | solvent | redox couple 4−/3− | 3−/2− | 2−/1− | 1−/0 | 0/1+ | 1+/2+ | 2+/3+ | 3+/4+ | $\Delta V^a$ | ref |
|---|---|---|---|---|---|---|---|---|---|---|---|
| $Fe_4(CO)_4Cp_4$ | $CH_3CN$ | | | | | −1.30 | 0.32 | 1.08 | | 2.38 | 2, 11 |
| $Fe_4S_4(NO)_4$ | $CH_2Cl_2$ | | | −0.65 | 0.13 | | | | | 0.78 | 4 |
| $Fe_4S_4(SR)_4$[b] | DMF | −1.88 | −1.23 | −0.07 | | | | | | 1.81 | 14 |
| $Fe_4S_4(SR)_4$[c] | $CH_2Cl_2$ | | −1.20 | −0.12 | | | | | | 1.18 | 14 |
| $Fe_4S_4Cp_4$ | $CH_3CN$ | | | | | −0.33 | 0.33 | 0.88 | 1.41 | 1.74 | 2, 3 |
| $Fe_4S_5Cp_4$ | $CH_3CN$ | | | −1.77 | −1.33 | −0.23 | 0.07 | 1.19 | | 2.96 | this work |

[a] $\Delta V$ is the difference between the highest and lowest observed half-wave potentials. [b] $R = C(CH_3)_2CH_2OH$. [c] $R$ = 2,4,6-($i$-Pr)$_3C_6H_2$.

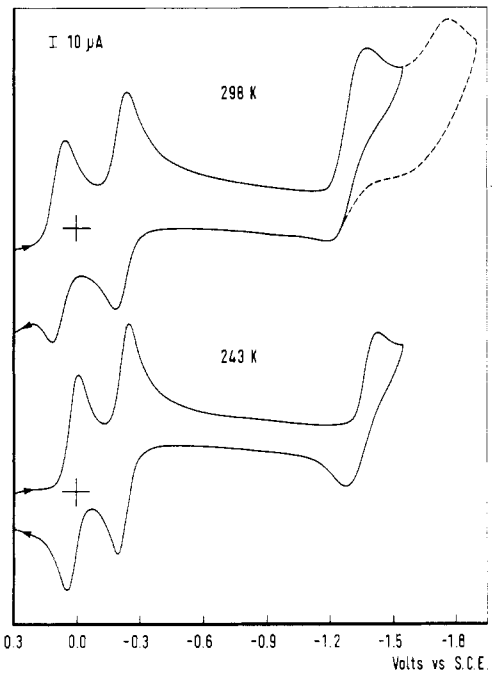


**Figure 2.** Redox behavior of the $Fe_4S_5Cp_4^{2+}$ compound in the potential range +0.3 to −1.90 V (vs. SCE) at two different temperatures. Other conditions are as for Figure 1.

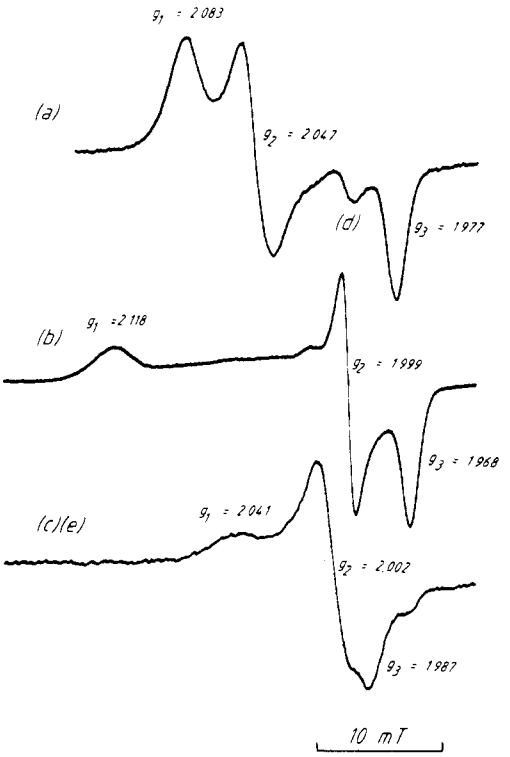


**Figure 3.** EPR frozen $CH_3CN$ solution spectra (ca. 40 K; ca. 9 GHz): (a) spectrum of $Fe_4S_5Cp_4^{3+}$; (b) spectrum of $Fe_4S_5Cp_4^{+}$; (c) spectrum of $Fe_4S_5Cp_4^{-}$; (d) spectrum of organic radical impurity at $g$ = 2.000; (e) spectrum obtained after subtraction of the $Fe_4S_4Cp_4^{-}$ signal.

EPR (vide infra), $[Fe_4S_5Cp_4]^-$ indeed appears to be the major component. Some decomposition of this species seems to occur, because in the EPR spectrum an additional minor signal is seen.

**EPR Spectra.** We have sought to improve the characterization of the paramagnetic, odd-electron-number oxidation states of this cluster by obtaining EPR data. X-Band spectra of frozen acetonitrile solutions of the monoanion, the monocation, and the trication, generated by controlled-potential enectrolysis, were recorded at 40 K and are shown in Figure 3.

All three signals are different from one another and each is characterized by three distinct $g$ values (reported in Table II). The spectra of $[Fe_4S_5Cp_4]^{3+}$ and $[Fe_4S_5Cp_4]^+$ (Figure 3a,b) show an additional signal at $g$ = 2.000 and 2.010, respectively, probably due to a minor paramagnetic unidentified component. The spectrum of $[Fe_4S_5Cp_4]^-$ (Figure 3c) was obtained after subtraction from the total spectrum (not shown) of a signal with $g$ values 2.124, 2.014, and 1.968.

The $[Fe_4S_5Cp_4]^{3+}$ and $[Fe_4S_5Cp_4]^+$ signals are easily saturated below 20 K and may be observed at higher temperatures than the $[Fe_4S_5Cp_4]^-$ signal, which is most visible below 40 K. This is indicative of a higher relaxation rate of the unpaired electron in the anion than in the cations. The spectrum of $[Fe_4S_5Cp_4]^-$ is also more isotropic than those of $[Fe_4S_5Cp_4]^+$ and $[Fe_4S_5Cp_4]^{3+}$.

In all three compounds, the $g$ values are characteristic of an overall electronic spin state $S = {}^1/_2$, which probably results from an antiferromagnetic coupling over the $Fe_4S_5$ core, as is usually the case in iron–sulfur systems.[10a] Upon reduction there is a decrease of the average $g$ value. This is consistent with an increased "ferrous" character of the iron atoms and is often seen in similar multinuclear Fe–S systems.[10]

**Oxidation States and Molecular Structure.** The electrochemical features observed for $[Fe_4S_5Cp_4]$ call for some remarks. First of all, the half-wave potentials of the $[Fe_4S_5Cp_4]^n$ series span over a larger range than observed for any other 4-Fe system, as evidenced by the $\Delta V$ values listed in Table III. The individual potential gaps $\Delta V_i$ between two successive redox steps are nearly constant in the case of $[Fe_4S_4Cp_4]$ ($\Delta V_i$ = 0.66, 0.55, 0.53 V). With $[Fe_4S_5Cp_4]$ on the contrary, there is a regular alternation of a small and of a large voltage separation ($\Delta V_i$ = 0.44, 1.10, 0.30, 1.12 V, these values being from the most reduced to the most oxidized state). One possible explanation could be that the small and large voltage gaps correspond to the abstraction of an elctron from a half-filled and completely filled HOMO, respectively, and that the successive HOMOs are located energetically further apart than in the case of $[Fe_4S_4Cp_4]^n$ ($n$ = 0 to 4+). Only quantitative MO calculations, however, will fully explain this observation.

Early reports[3,11] on $[Fe_4(CO)_4Cp_4]$ and $[Fe_4S_4Cp_4]$ claimed the existence of the 1− to 2+ and 1− to 3+ oxidation states, respectively. However, as pointed out by a reviewer, it is communicated in a recent review[2] that these assignments were in error, and they should be 0 to 3+ and 0 to 4+, respectively. Indeed, our recently measured reaction entropy values for the redox

(10) (a) Cammack, R.; Dickson, D. P. E.; Johnson, C. E. In *Iron-Sulfur Proteins*; Lovenberg, W., Ed.; Academic: New York, 1977; Vol. III, p 283. (b) Christou, G.; Garner, C. D.; Drew, M. G. B.; Cammack, R. *J. Chem. Soc., Dalton Trans.* **1981**, 1550.

(11) Ferguson, J. A.; Meyer, T. J. *J. Am. Chem. Soc.* **1972**, *94*, 3409.

processes of $[Fe_4S_4Cp_4]$ (and some analogous compounds) are in agreement with the now proposed $n = 0$ to 4+ oxidation states.[12] The new assignments made in the case of $[Fe_4(CO)_4Cp_4]$, however, are not supported by our entropy data.

Apart from the small differences in half-wave potentials for $[Fe_4S_5Cp_4]$ and $[Fe_4S_4Cp_4]$, the main difference in redox behavior is that $[Fe_4S_5Cp_4]$ can be reduced to the 1- and 2- ion. The oxidation to the 4+ ion of $[Fe_4S_5Cp_4]$ is probably outside the potential window of our experiments.

Thus, our results demonstrate that $[Fe_4S_5Cp_4]$ exists at six different oxidation states and that the cluster structure is kept intact during five of these ($n$ = 1- to 3+). This is quite noteworthy, since few species possess this property, and the addition or subtraction of more than one electron usually leads to a structural disruption. So far, $[Fe_4S_4Cp_4]^n$[2,3] and $[Fe_4S_4(SR)_4]^n$ (R = $C_6H_5$, $C(CH_3)_2CH_2OH$, 2,4,6-($i$-Pr)$_3C_6H_2$)[13,14] are the only other tetranuclear Fe clusters known to exist at five and four different oxidation states, respectively. Ferrocene-type compounds, such as 1,1′-quaterferrocene[15] and $(C_{10}H_8)(C_6Me_6)Fe_2^n$ ($n$ = 2+ to 2-),[16] have also been reported to exhibit five oxidation states.

The structural data (by X-ray diffraction[6,7] and/or Fe-EXAFS[17]) for $[Fe_4S_5Cp_4]$ in its neutral, monopositive and dipositive states being available, it was of interest to correlate the observed structural variations in the $Fe_4S_5$ core with the successive reductions and to predict its geometry in the (as yet) nonisolated mono- and dianions. The major changes encountered are primarily reflected in the Fe–Fe interactions. The averaged Fe–Fe distances, presented in Table II, increase steadily upon reduction (from 2.63 to 2.78 and then to 2.96 Å). A more detailed analysis shows that, from the dication to the monocation and then to the neutral cluster, one of the two bonding Fe–Fe interactions weakens as the bonding length increases from 2.63 to 2.91 and then to 3.31 Å, while the other remains approximately constant (2.61 to 2.65 Å). In other words, the addition of the first and then of the second electron causes the lengthening of one of the Fe–Fe distances until it stretches well beyond the 3-Å limit. If the same trend persists when adding more electrons, one can assume that, after addition of a fifth electron to form $[Fe_4S_5Cp_4]^{2-}$, there will be no Fe–Fe bonding interactions left. This coincides with the breakdown of the $Fe_4S_5$ core structure, since we observed that $[Fe_4S_5Cp_4]^{2-}$ is unstable and expels sulfur. Metal–metal interactions therefore appear to play an important role in the stability of the $[Fe_4S_5Cp_4]$ series and its capability of "adsorbing" several electrons without undergoing any major structural changes.

**Acknowledgment.** We thank Professor J. J. Steggerda for his stimulating interest in this work.

(12) Blonk, H. L.; Berkelmans, J. F. J.; van der Linden, J. G. M., in preparation.
(13) Pickett, C. J. *J. Chem. Soc., Chem. Commun.* **1985**, 323.
(14) (a) Mascharak, P. K.; Hagen, K. S.; Spence, J. T.; Holm, R. H. *Inorg. Chim. Acta* **1983**, *80*, 157. (b) O'Sullivan, T.; Miller, M. *J. Am. Chem. Soc.* **1985**, *107*, 4096.
(15) Brown, G. M.; Meyer, T. J.; Cowan, D. E.; LeVanda, C.; Kaufman, F.; Roling, P. V.; Rausch, M. D. *Inorg. Chem.* **1975**, *14*, 506.
(16) Desbois, M. H.; Astruc, D.; Guillin, J.; Mariot, J. P.; Varret, F. *J. Am. Chem. Soc.* **1985**, *107*, 5280.
(17) Diakun, G.; Jordanov, J., submitted for publication.

Contribution from the Dipartimento di Chimica Inorganica e Struttura Molecolare, Università di Messina, 98100 Messina, Italy, and Dipartimento di Chimica, Università di Siena, 53100 Siena, Italy

# Synthesis, X-ray Crystal Structure, and Electrochemical Properties of the $Rh_2^{4+}$ Complex $Rh_2(form)_4$ (form = *N,N′*-Di-*p*-tolylformamidinate Anion)

Pasquale Piraino,*† Giuseppe Bruno,† Sandra Lo Schiavo,† Franco Laschi,‡ and Piero Zanello*‡

*Received August 5, 1986*

The reaction of the dirhodium(II) mixed-ligand complex $Rh_2(form)_2(O_2CCF_3)_2(H_2O)_2$ (form = *N,N′*-di-*p*-tolylformamidinate anion) with free *N,N′*-di-*p*-tolylformamidine (mole ratio 1:4) leads to the formation of the complex $Rh_2(form)_4$ (**1**) in excellent yield. The complex was characterized by a single-crystal X-ray diffraction analysis, crystallizing in the space group $Pn\bar{3}n$, with $a$ = 20.990 (2) Å, $V$ = 9248 Å$^3$, $Z$ = 6, $R$ = 0.036, and $R_w$ = 0.0378. The Rh–Rh [2.4336 (4) Å] and the Rh–N [2.050 (5) Å] bond distances are well in the range observed for this class of compounds. The molecule is in a staggered conformation, with N–Rh–Rh–N torsion angles of 16.7 (2)°. Complex **1** reacts with carbon monoxide, giving the monocarbonyl adduct $Rh_2(form)_4(CO)$ (**2**), characterized by elemental analysis and IR, $^{13}C$ NMR, and electrochemical measurements. Unlike other dirhodium(II) carbonyl derivatives, **2** is remarkably stable. In the $^{13}C$ NMR spectrum a dramatic upfield shift is seen for the carbonyl resonance ($\delta$ 144.06); the IR spectrum shows $\nu$(CO) at 2040 cm$^{-1}$. These data coupled to electrochemical measurements suggest that the $\pi$ back-bonding is reasonably strong in **2**. The electrode behavior of **1** has been investigated in different nonaqueous solvents. Complex **1** undergoes two anodic redox changes, Rh(II)–Rh(II)/Rh(II)–Rh(III) (reversible) and Rh(II)–Rh(III)/Rh(III)–Rh(III) (irreversible), and one cathodic change, Rh(II)–Rh(II)/Rh(II)–Rh(I) (irreversible), under cyclic voltammetry. The ESR spectrum at 100 K of the species $[Rh_2(form)_4]^+$ displays $g_\perp$ = 2.062 and $g_\parallel$ = 1.957. The $g_\parallel$ is split into a 1:2:1 triplet by two equivalent rhodium nuclei ($A_\parallel = 18.9 \times 10^{-4}$ cm$^{-1}$). The generated Rh(II)–Rh(III) species is quite stable, and it belongs to the completely delocalized "class III" (Robin–Day) mixed-valent derivatives.

## Introduction

The chemistry of the complexes containing the $Rh_2^{4+}$ core, represented by the parent complex $Rh_2(O_2CCH_3)_4$, was dominated until recently by complexes containing four carboxylates as bridging ligands, known as the "lantern" structure.[1] $Rh_2^{4+}$ complexes containing the N–C–O groups, $[Rh_2(mhp)_4$ (mhp = 6-methyl-2-hydroxypyridinato),[2] $Rh_2(RNOCR')_4$ (R = $C_6H_5$; R′ = $CH_3$)[3]], the N–C–N groups $[Rh_2(PhNpyr)_4$,[4] $Rh_2(N_2R_2CR)_4$[5]], or the pyrazolate anion[6] $[Rh_2(3,5\text{-}Me_2pz)_4]$ were isolated recently.

For all of the above-mentioned $Rh_2^{4+}$ complexes, the observed chemical reactivity is limited to introduction of an axially coordinated ligand. In some cases,[4] this is prevented by the steric

(1) (a) Felthouse, T. R. *Prog. Inorg. Chem.* **1982**, *20*, 109. (b) Boyer, E. B.; Robinson, S. D. *Coord. Chem. Rev.* **1983**, *50*, 109. (c) Cotton, F. A.; Walton, R. A. *Multiple Bonds between Metal Atoms*; Wiley-Interscience: New York, 1982; p 311.
(2) (a) Berry, M.; Garner, C. D.; Hillier, I. H.; Macdowell, A. A.; Clegg, W. *J. Chem. Soc., Chem. Commun.* **1980**, 494. (b) Cotton, F. A.; Felthouse, T. R. *Inorg. Chem.* **1981**, *20*, 584.
(3) Duncan, J.; Malinski, T.; Zhu, T. P.; Hu, Z. S.; Kadish, K. M. *J. Am. Chem. Soc.* **1982**, *104*, 5507.
(4) Tocher, D. A.; Tocher, J. H. *Inorg. Chim. Acta* **1985**, *104*, L15.
(5) Le, J. C.; Chavan, M. Y.; Chau, L. K.; Bear, J. L.; Kadish, K. M. *J. Am. Chem. Soc.* **1985**, *107*, 7195.
(6) Barron, A. R.; Wilkinson, G.; Motevalli, M.; Hursthouse, M. B. *Polyhedron* **1985**, *4*, 1131.

† Università di Messina.
‡ Università di Siena.

0020-1669/87/1326-2205$01.50/0 